ACTIVE MAGNETIC BEARINGS APPLIED TO INDUSTRIAL COMPRESSORS

R. G. Kirk
Virginia Polytechnic Institute and State University
Blacksburg, Virginia 24061

J. F. Hustak
K. A. Schoeneck
Dresser-Rand Turbo Division
Olean, New York

SUMMARY

The design and shop test results are given for a high-speed eight-stage centrifugal compressor supported by active magnetic bearings. A brief summary of the basic operation of active magnetic bearings and the required rotor dynamics analysis are presented with specific attention given to design considerations for optimum rotor stability. The concerns for retrofits of magnetic bearings in existing machinery are discussed with supporting analysis of a four-stage centrifugal compressor. The current status of industrial machinery in North America using this new support system is presented and recommendations are given on design and analysis requirements for successful machinery operation of either retrofit or new design turbomachinery.

INTRODUCTION

A new technology in the form of active magnetic bearings (AMB) is being introduced into the marketplace for use on individual turbomachinery. The features of this technology, when applied to turbocompressor design, result in several economic, performance, and versatility improvements unavailable to the industry at the present time. Active magnetic bearings used in conjunction with dry gas seals and dry couplings now enable both the manufacturer and user to think in terms of oil-free centrifugal compressors.

Patent activity on passive, active, and combination magnetic bearing systems spans 150 years. The bulk of the initial investigations centered on permanent magnetic systems because they were easy to fabricate. It was later shown, however, that a passive magnetic suspension for three axes of displacement is unstable. This theory, first stated by Earnshaw (1) in 1842 is still valid today. The first totally active magnetic suspension system was described (2) and documented in a patent issued in 1957, but application to practical design conditions were not possible due to a lack of suitable electronic circuitry to switch the large DC currents required. In 1970, a totally active magnetic suspension system was developed for a communications satellite and in 1976, a new company was formed to further develop and commercially market active magnetic bearing systems internationally (3,4).

PRINCIPLE OF ACTIVE MAGNETIC BEARING OPERATION

The AMB is composed of two major mechanical parts consisting of the rotor and the stator. Both are made of ferromagnetic laminations. The rotor laminations are placed on the machine shaft at the selected journal location. The stator laminations are slotted and include windings to provide the magnetic levitation and position control. For each degree of freedom, two electromagnets are required since they operate by attraction only. Figure 1 shows the stator laminate construction of a radial bearing with the rotor laminate sleeve in the background.

Rotor position is monitored by sensors, and this signal is compared to a nominal reference signal with a closed loop controller which supplies a command signal to the power amplifier. These amplifiers provide power to the electromagnets to resist rotor movement from the nominal position. The design of the control loop gives the option to select the effective bearing damping and stiffness. The details of this design procedure are not the subject of this paper but the values of stiffness and damping must be carefully selected to give the rotor system the desired optimum dynamic response and stability.

This design concept can be applied to both radial and axial thrust bearings to give total control of a rotating rotor system. The load capacity of the AMB using standard materials can be made equal to standard fluid-film bearing designs. The overload condition for the AMB is controlled by auxiliary bearings which must be designed to provide rotor constraint in the event of system power failure or momentary transient overload.

The many advantages and detailed design requirements for the AMB are discussed in greater detail by Haberman (3,4). The application of the AMB to industrial compressors with proper evaluation of the rotor dynamic response and stability is essential for success of this new technology. This latter concern will be addressed in the following discussion.

DEVELOPMENT CENTRIFUGAL COMPRESSOR WITH AMB

Figure 2 is a view of an eight-stage, horizontally split, back-to-back centrifugal compressor equipped with magnetic radial and thrust bearings and gas seals on test at the authors' former company, 1980. The eight-stage rotor housed inside the compressor, originally designed to run at 167 Hz (10,000 rpm) on hydrodynamic bearings, has since operated successfully for 750 hours at speeds up to 217 Hz (13,000 rpm) on magnetic bearings. The compressor is shown attached to two closed loops constructed for the purpose of operating the rotor in a pressurized environment over a wide range of pressures and flows from choke to surge.

One unique feature of this compressor was the installation of the thrust and journal bearings located on the free end of the rotor directly into the gas (nitrogen) pressurized environment, thereby eliminating the need for one shaft seal. To illustrate the concept of a nonlubricated centrifugal compressor, a gas seal was chosen as the main shaft seal on the coupling end of the rotor. Table 1 summarizes some of the important design features of the eight-stage back-to-back rotor while Fig. 3 illustrates the appearance of the fully assembled test rotor.

Before power is applied to the bearings, the rotor is supported on two auxiliary ball bearings located in close proximity to the AMB. The clearance between the rotor and the inner race of the ball bearing is selected to prevent rotor contact with the AMB pole pieces or the internal seals of the compressor while the rotor is at rest or during an emergency shutdown. Typical shaft radial clearances in the AMB, internal seals, and auxiliary bearing inner race are 0.3 mm (0.012 in.), 0.254 mm (0.010 in.), and 0.15 mm (0.006 in.), respectively. When power is applied to the electronic controls, the electromagnets levitate the rotor in the magnetic field and rotation of the driving source, such as a motor or turbine, can be started. The sensors and control system regulate the strength and direction of the magnetic fields to maintain exact rotor position by continually adjusting to the changing forces on the rotor. Should both the main and redundant features of the AMB fail simultaneously, the auxiliary bearings and rotor system are designed to permit safe deceleration.

Magnetic bearing stiffness and damping properties are controlled by a PID (Proportional, Integral, Derivative) analog control loop that allows some flexibility for adjustment. The stiffness and damping characteristics are axi-symmetric, i.e., identical in both the horizontal and vertical directions. The resultant dynamic bearing stiffness, KD, is a complex number represented by the vectorial summation of a "real" stiffness component (K) and an "imaginary" stiffness component ($c\omega$).

$$KD = \sqrt{K^2 + (c\omega)^2} \tag{1}$$

The phase relationship (α) between the "real" (K) and "imaginary (cw) components is given by

$$\alpha = \arctan (c\omega/K) \tag{2}$$

where K = static real stiffness (N/m), ω = angular velocity of journal vibraton (sec^{-1}). Variation of the phase angle ranges from 0 to 90 degrees with typical values in the 30 to 40 degree range. Adjusting the amount of bearing damping is accomplished by changing the passive elements of the compensation circuit in the PID control loop. The amount of gain applied to the circuit through a potentiometer provides a proportional increase in the resultant dynamic stiffness, KD.

The undamped critical speed map shown in Fig. 4 compares the standard fluid film bearing/oil seal design to the magnetic bearing/gas seal design for the 8-stage development compressor. The magentic bearing design increased the first rigid bearing mode by reducing the bearing span but decreased the second, third, and fourth modes due to the additional weight of the ferromagnetic journal sleeves and the larger diameter thrust collar. Superimposed on this map are the stiffness and damping properties of the electromagnetic bearings as a function of rotor speed. For a design speed of 167 Hz (10,000 rpm), Fig. 4 indicates the rotor would have to pass through three critical speeds and operate approximately 20 percent above the third critical and 40 percent below the fourth critical. Furthermore, since both the first and second criticals are rigid body modes, only a significant response at approximately 133 Hz (8000 rpm) would be expected as the rotor passed through its third (free-free mode) critical. Subsequent unbalance forced response calculations verified these expectations with acceptable operations of the compressor to 233 Hz (14,000 rpm) (see Figs. 5 and 6).

The damping required for optimum stability may be arrived at by plotting the systems' calculated damped natural frequencies versus growth factors (5), (6), (7), For the first mode stiffness of 22.8 N/μm (130,000 lb/in), Fig. 7 shows the movement of the eigenvalues as the bearing damping varies. Increased damping levels cause the first and second modes to become critically damped. The third mode

increases in stability up to a point of 87.7 N-s/mm (501 lb-s/in.) but then decreases as damping is increased further. Since the first and second modes become critically damped, a second study was undertaken to determine if the third mode would go unstable at its corresponding stiffness of 40.1 N/μm (229,000 lb/in). The results of that analysis are presented in Fig. 8 and indicate the third mode becomes critically damped as the damping is increased, while the first mode damping would be at an optimum for 112.9 N-s/mm (645 lb-s/in.). The behavior of the first and third modes, resulting from the increase in bearing stiffness, is similar to results presented by Lund (5). These results indicate that a level of 70-87.5 N-s/mm (400-500 lb-s/in.) would be ideal for all modes up to and including the fourth.

The stiffness and damping characteristics for the magnetic bearing are given in Fig. 9. Active magnetic bearings have an important difference when compared to conventional fluid film bearings. Typical preloaded five-shoe tilt-pad bearings have characteristics generated predominantly by operating speed, with little influence from nonsynchronous excitations (8). The active magnetic bearing characteristics, shown in Fig. 9, are dependent on the frequency of excitation regardless of operating speed. For a given stiffness value selected to minimize unbalance forced response, the damping characteristics at subsynchronous excitation frequencies can be specified to assure optimum stability (3), (4).

The test program outlined for the compressor was directed toward confirming the analytical predictions for the dynamic behavior of the rotor and experimentally demonstrating the reliability of the complete system under typical operating conditions. The fully assembled compressor was installed on the test stand and operated at a maximum discharge pressure of 4.1 MPa (600 psig) with speeds up to 217 Hz (13,000 rpm). The results for a deceleration as recorded at the bearing probe locations are given in Figs. 10 and 11. The test results indicate well-damped rotor responses at 67 Hz (4000 rpm) and 133 Hz (8000 rpm). In comparison, the synchronous response to unbalance shown in Figs. 5 and 6 displays well-damped rotor response at 67 Hz (4000 rpm) and 133 Hz (8000 rpm). The amplitude of vibration is difficult to predict since the actual rotor unbalance configuration is made up of varying amounts of unbalance at different axial locations along the rotor. The predicted peak response frequencies are considered to be in good agreement with the test results.

DESIGN EVALUATION OF A FIELD RETROFIT

The economic advantages of gas seals and/or magentic bearings have prompted interest in retrofit of existing units. For either retrofit or new machinery, attention must be given to placement of critical speeds for both main and backup bearings, response sensitivity, and overall stability considerations. The preliminary design study for a four-stage high-speed centrifugal compressor will illustrate in more detail the parameters that must be considered for total system dynamic analysis. The basic design parameters for this rotor are indicatd in the second column of Table 1.

The undamped critical speed map for the four-stage compressor and dynamic stiffness values are shown in Figs. 12 and 13. The magnetic bearing stiffness is positioned such that the compressor must pass through three critical speeds before reaching a maximum continuous operating speed of 241.7 Hz (14,500 rpm). Due to the rigid body nature of the second and third modes, the actual damped critical speeds will occur from the first and fourth modes. The frequencies at which these modes respond, shown in Figs. 14 and 15, are 71.7 Hz (4300 rpm) and 305 Hz (18,300 rpm).

A plot of the systems calculated damped natural frequencies versus growth factor for a constant first mode stiffness of 15.1 N/μm (86,300 lb/in.) is shown in Fig. 16. The first forward mode typically goes unstable while the second and third modes become critically damped as the bearing damping is increased. For this compressor design, the first mode increases in stability as the damping increases up to 39.4 N-s/mm (225 lb-s/in.) but then decreases as the damping is increased further. The damping value initially supplied, 24.5 N-s/mm (140 lb-s/in.), should be increased by 61 percent based on the results of this analysis.

The optimum damping for stabiity was also calculated by an approximate method using the modal mass, rigid bearing critical frequency, and bearing stiffness (see Table 1). The equation from Ref. (9) can be written as follows (valid for high $\bar{K}$ ratios):

$$C_o = 2.893 \times 10^{-2} N_{cr} \left[M_m + \frac{4.98 \times 10^5 K_b}{N_{cr}^2} \right] \quad (3)$$

Example for four-stage first mode:

$$C_o = 2.893 \times 10^{-2} \times (90.39) \times (649 + (4.98 \times 10^5) \times (15.1)/(90.39)^2)$$

$$= 45.4 \text{ N-s/mm}$$

This quick calculation gives an answer 15 percent higher than the lengthy optimum damping method used in Fig. 16.

Figure 17 shows a comparison of stability versus aerodynamic excitation between the conventional fluid film design and the magnetic bearing retrofit design. The increase in stability due to the magnetic bearing and dry gas seal design moves the log dec from near zero to a value of 1.41.

Current Status of Active Magnetic Bearings

The application of magnetic bearings for industrial installations in North America has progressed to the point that both retrofit and new, original design applications have been initiated with successful operation on test and in the field. Table 2 shows the current status of new and retrofit turbomachinery in North America. The use of this new method of turbomachinery support and control has not been totally free of test stand problems. Machinery must withstand extremes of temperatures for various design applciations which must be properly evaluated to assure adequate bearing materials selection. In addition, loading from rotor system balance variations due to initial build and transient excitation resulting from process upsets must be accounted for in the initial design considerations.

These potential problems make the design prediction capability and initial design studies for rotor dynamics analysis just as important for AMB as it has been for machinery supported on fluid-film bearings.

CONCLUSIONS AND RECOMMENDATIONS

The capability of an active magnetic bearing system to support a flexible turbocompressor rotor and simultaneously influence its vibrations has been successfully demonstrated. During 750 hours of accumulated operating time for the development compressor equipped with active magnetic bearings, the following observations were made:

1. The rotor behaved in a stable manner at all times when accelerating/decelerating through its first three critical speeds.
2. The rotor behaved in a stable manner while undergoing surge cycles at maximum discharge pressure.
3. The magnetic bearings were able to suppress rotor amplitude to avoid contact between rotational and stationary components through the first three modes up to a speed of 271 Hz (13,000 rpm). Speeds beyond this point were limited by impeller stress considerations.

The following recommendations can be made for the design and analysis of magnetic bearing suspension turbomachinery:

1. Bearing stiffness should be selected by evaluation of shaft stiffness ratio with typical placement at the beginning of the third mode ramp on the undamped critical speed map.
2. Bearing damping should be specified to give the optimum stability with consideration given to all modes below maximum operating speed.
3. Consideration must be given to the next mode above operating speed (typically the fourth mode) to avoid interference between operating speeds and system natural frequencies.
4. The machinery must be engineered such that the shaft critical speeds are at least 10 percent lower or higher than any continuous operating speed when the rotor system is assumed to be operating on the auxiliary bearings.

ACKNOWLEDGMENTS

The authors wish to thank Mr. Howard Moses and Mr. David Weise of Magnetic Bearings Incorporated, Radford, VA for their assistance in the preparation of this paper and the permission to publish the information given in Table 2.

REFERENCES

1. Earnshaw, S., "On the Nature of the Molecular Forces," Trans. Cambridge Phil. Soc. 7, 97-112, 1842.

2. Tournier, M., and Laurenceau, P., "Suspension magnetique d'une maquette en soufflerie," La Recherche Aeronautique 7-8, 1957.

3. Haberman, H., "The Active Magnetic Bearing Enables Optimum Damping of Flexible Rotors," ASME Paper 84-GT-117.

4. Haberman, H., and Brunet, M., "The Active Magnetic Bearing Enables Optimum Control of Machine Vibrations," ASME Paper 85-GT-22, Presented at Gas Turbine Conf., Houston, TX, March 18-21, 1985.

5. Lund, J. W., "Stability and Damped Critical Speeds of a Flexible Rotor in Fluid-Film Bearings," J. of Eng. for Industry, Trans. ASME, Series B. 96, 2, pp. 509-517, May (1974).

6. Bansal, P., and Kirk, R. G., "Stability and Damped Critical Speeds of Rotor-Bearing Systems," J. of Eng. for Industry, Trans. ASME, Series B, 98, 1, pp. 108, February (1976).

7. Kirk, R. G., "Stability and Damped Critical Speeds--How to Calculate and Interpret the Results," CAGI Technical Digest, 12, 2, pp. 1-14 (1980).

8. Wilson, B. W., and Barrett, L. E., "The Effect of Eigenvalue-Dependent Tilt Pad Bearing Characteristics on the Stability of Rotor-Bearing Systems," Univ. of Virginia, Report No. UVA643092/MAES5/321, January 1985.

9. Barrett, L. E. Gunter, E. J., and Allaire, P. E., "Optimum Bearing and Support Damping for Unbalance Response and Stability of Rotating Machinery," Trans. ASME, J. of Eng. for Power, pp. 1-6 (1978).

Table 1--Centrifugal Compressor Design Parameters and Nomenclature

Parameter, Nomenclature SI Units (US Units)	Eight-Stage		Four-Stage	
Operating Speed, N, Hz, (rpm)	217.7	(13 000)	241.7	(14 500)
Total Weight, W, N, (lb)	3678	(827)	1237	(278)
Bearing Span, mm, (in.)	1269	(49.97)	886	(34.88)
Shaft Length, mm, (in.)	1902	(74.90)	1253	(49.32)
Coupling End Overhang, mm, (in.)	304.8	(12)	184.9	(7.28)
Shaft Stiffness K_s, N/μm ,(lb/in.)	61.1	(3.49E5)	21.4	(1.22E5)
Bearing Stiffness @ MCOS, K_b, N/μm ,lb/in.	63.9	(3.65E5)	28	(1.60E5)
Stiffness Ratio, $\overline{K}$, Dim., (Dim.)	0.74	(0.74)	1.41	(1.41)
Mid-Span Diameter, mm, (in.)	123.9	(4.88)	76.2	(3)
Journal Diameter, mm, (in.)	187.5	(7.38)	93	(3.66)
First Rigid Bearing Critical, N_{cr}, Hz,(rpm)	92.52	(5551)	90.39	(5423)
First Peak Response Speed, FPS1, Hz, (rpm)	129.5	(7700)	71.67	(4300)
Second Peak Response Speed, FPS2, Hz, (rpm)	271.7	(16,300)	305	(18 300)
First Mode Modal Mass, M_m, N, (lb_m)	1775.	(399)	649	(146)
Bearing Stiffness @ N_1, K_{b1}, N/μm ,(lb/in.)	22.8	(1.30E5)	15.1	(8.63E4)
Optimum Damping (9), C_o, N-s/μm , (lb-s/in.)	9.18E-2	(524)	4.54E-2	(259)

Note: Values are given in both SI and US customary units. The measurements and calculations were made in US customary units.

Table 2 AMB Industrial Compressor Applications in North America

MACHINE	TYPE	SERVICE	DUTY	COMM	ROTOR WEIGHT (lb) N	THRUST LOAD (lb) N	SPEED (rpm) Hz	JOURNAL DIAMETER (in) cm	DRIVER RATING (HP) kw	OPERATING HOURS (*)
MTA-824BB	CENT COMP	DEVELOP-MENT	INTERMIT	1980	(850) 3778	(3150) 14 000	(13 000) 217	(7.5) 19.0	(5360) 3997	750
CDP-230	CENT COMP	PIPELINE	SEASONAL	1985	(3200) 14224	(12 000) 52 340	(5250) 87.5	(10.6) 26.9	(12 800) 9545	6800
CDP-416	CENT COMP	PIPELINE	SEASONAL	1986	(280) 1245	(3370) 14 980	(14 500) 242	(3.7) 9.4	(4250) 3095	6700
IB26	CENT COMP	PIPELINE	CONTINUOUS	1986	(780) 3467	(4050) 18 000	(11 000) 183	(6.5) 16.5	(5500) 4101	4800
IB26	CENT COMP	PIPELINE	CONTINUOUS	1987	(780) 3467	(4050) 18 000	(11 000) 183	(6.5) 16.5	(5500) 4101	300
CBF-842	CENT COMP	REFINERY	CONTINUOUS	1987	(1420) 6312	(4590) 20 403	(10 250) 171	(6.0) 15.2	(4500) 3356	750
5P2	CENT COMP	PIPELINE	SEASONAL	NEW	(1540) 6845	(5500) 24 448	(7140) 119	(6.0) 15.2	(16 600) 12 379	

*AMB Cabinet operating hours as of December 15, 1987

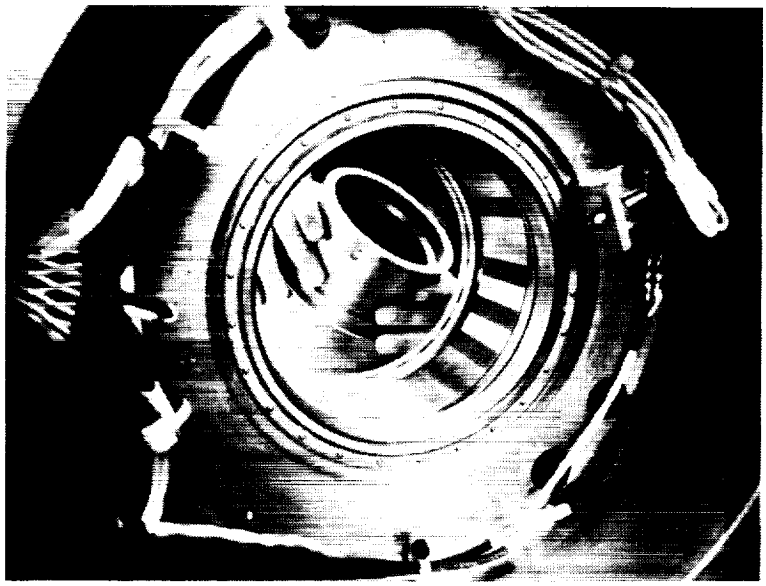

Figure 1. Active magnetic bearing stator with rotor sleeve in background.

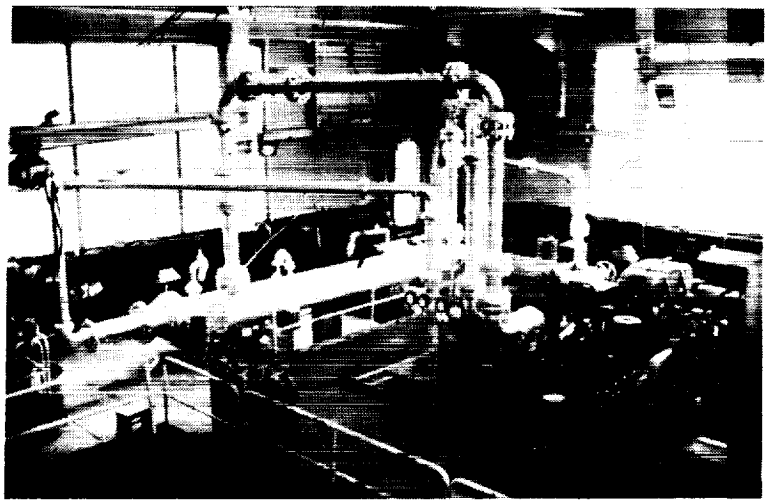

Figure 2. Eight-stage development compressor test setup.

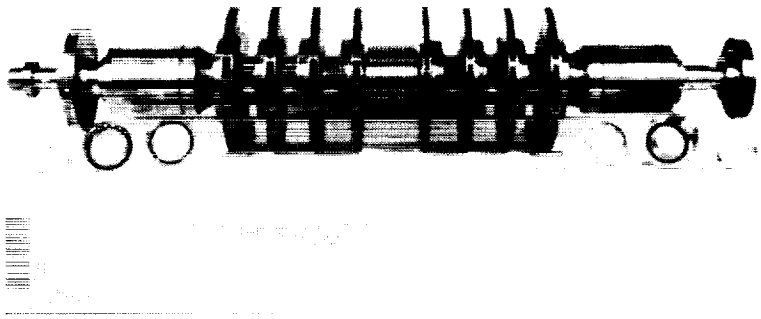

Figure 3. Eight-stage development compressor rotor.

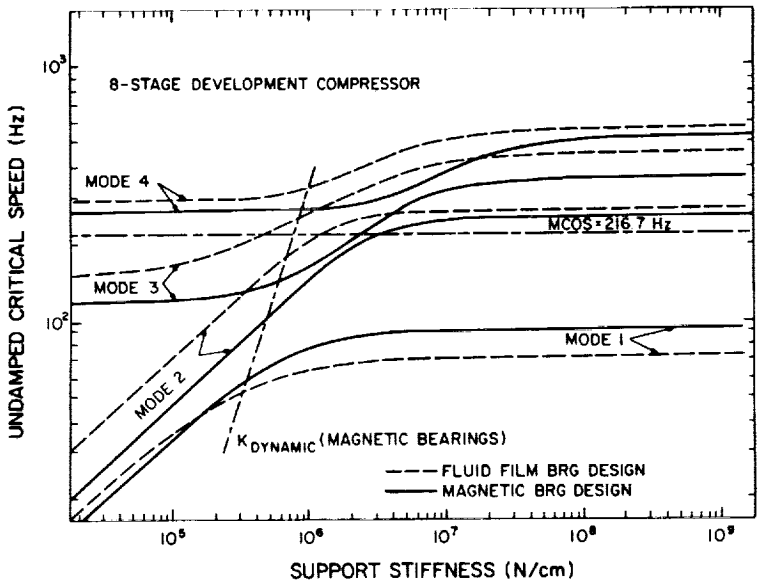

Figure 4. Eight-stage development compressor undamped critical speed map.

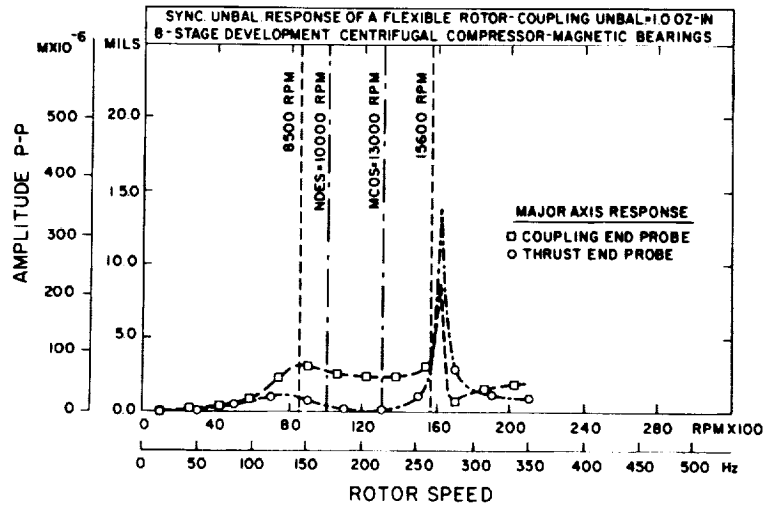

Figure 5. Eight-stage development compressor synchronous response to coupling unbalance.

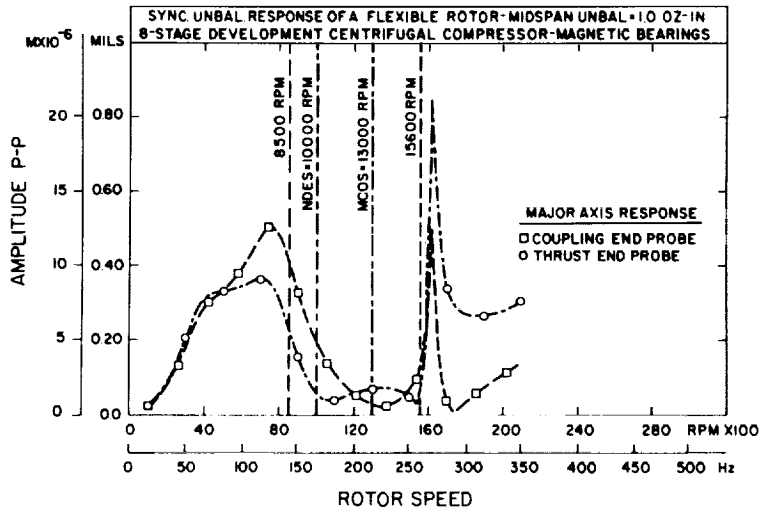

Figure 6. Eight-stage development compressor synchronous response to midspan unbalance.

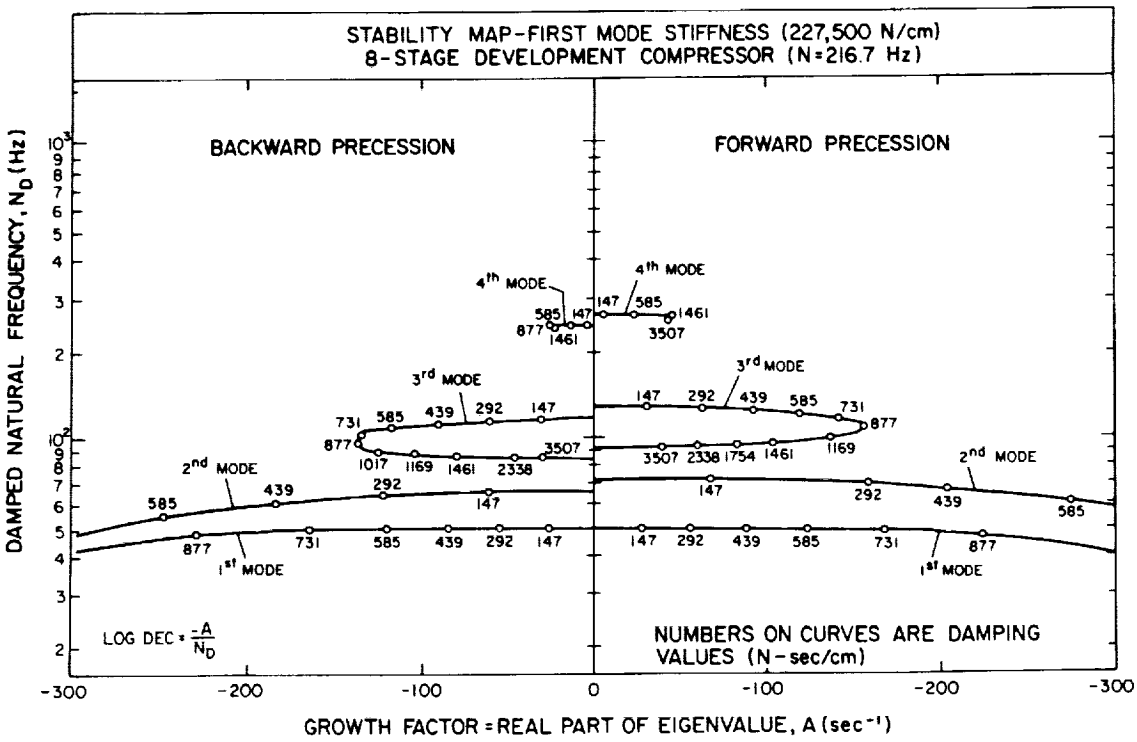

Figure 7. Eight-stage development compressor stability map for first mode stiffness.

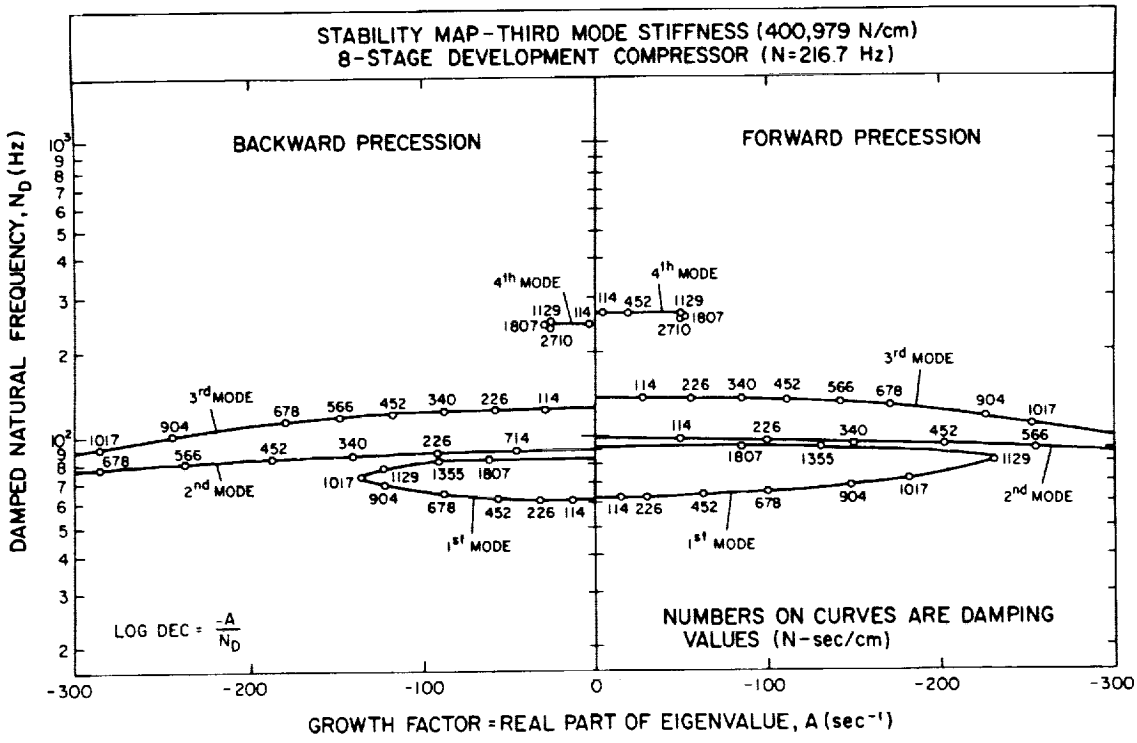

Figure 8. Eight-stage development compressor stability map for third mode stiffness.

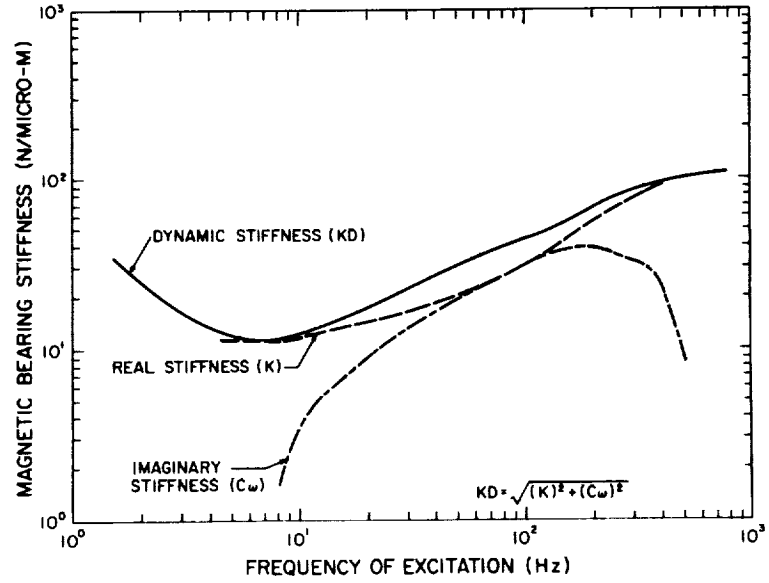

Figure 9. Eight-stage development compressor magnetic bearing characteristics.

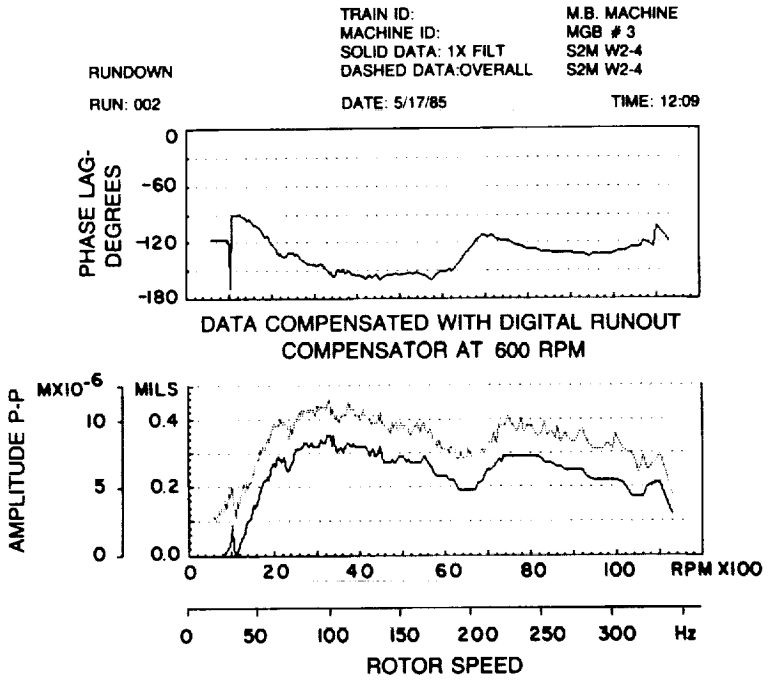

Figure 10. Eight-stage development compressor coupling end response from test results.

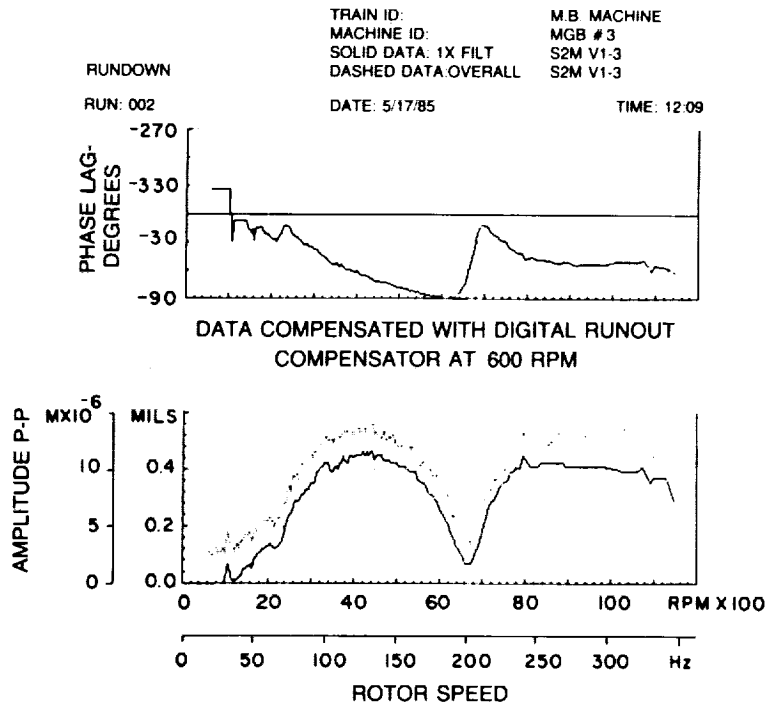

Figure 11. Eight-stage development compressor thrust end response from test results.

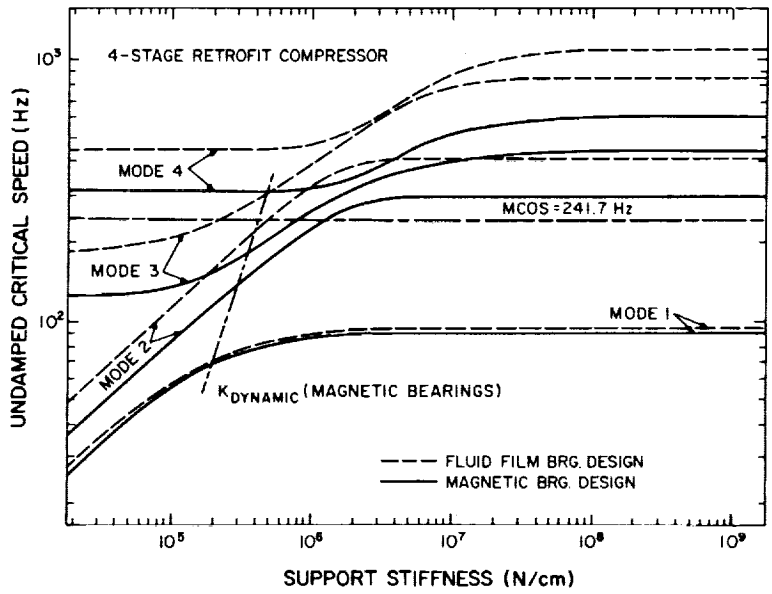

Figure 12. Four-stage retrofit compressor undamped critical speed map.

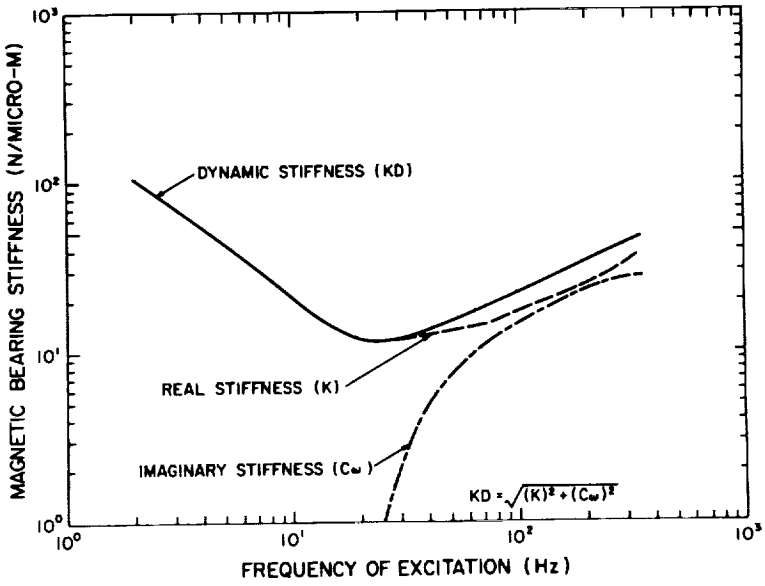

Figure 13. Four-stage retrofit compressor magnetic bearing characteristics.

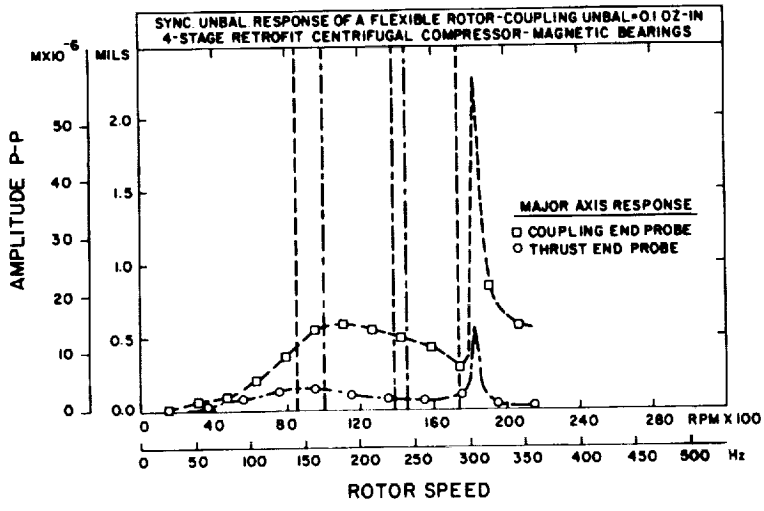

Figure 14. Four-stage retrofit compressor synchronous response to coupling unbalance.

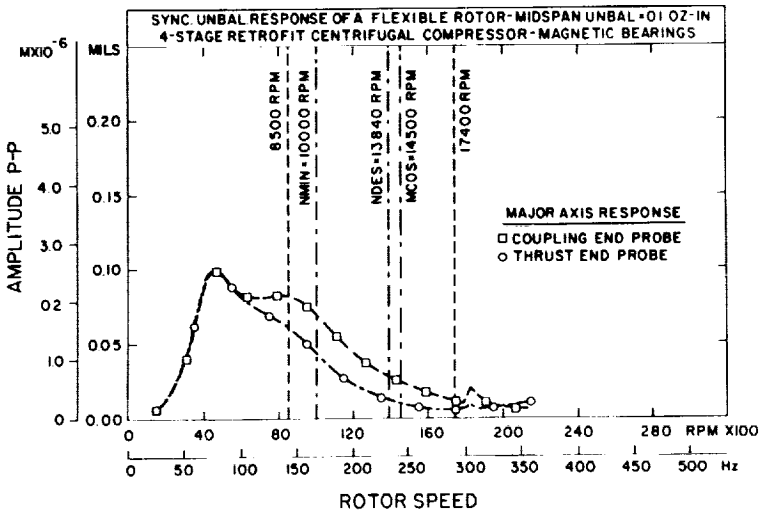

Figure 15. Four-stage retrofit compressor synchronous response to mid-span unbalance.

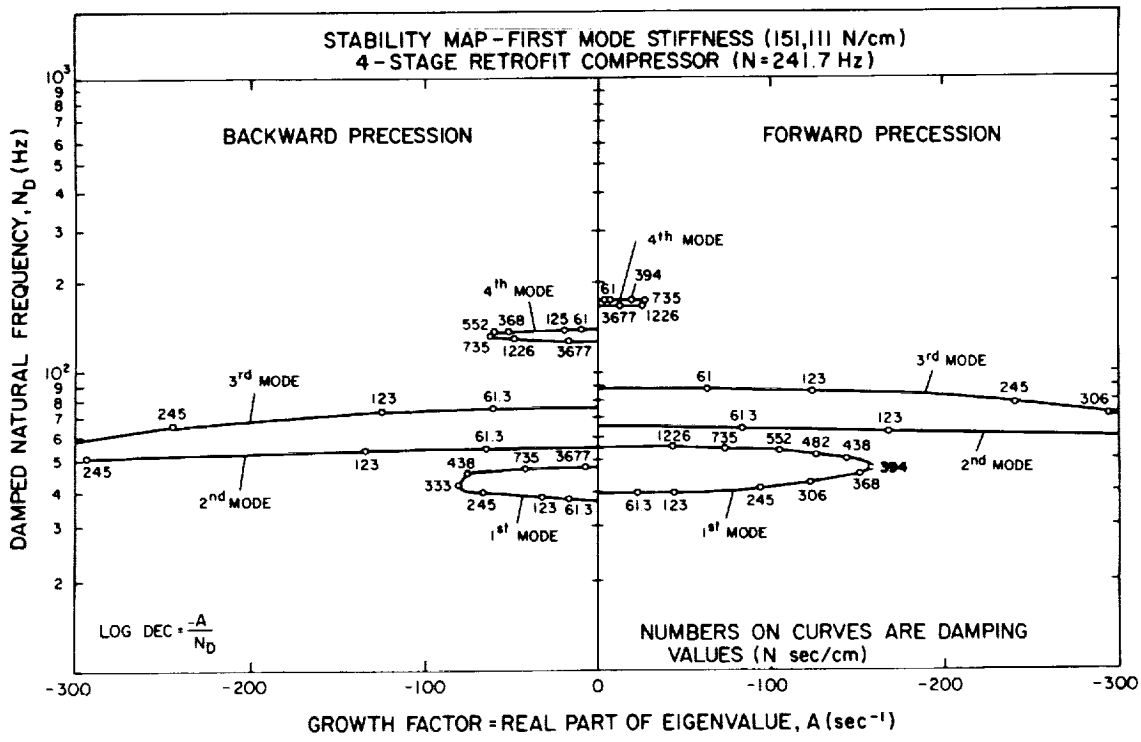

Figure 16. Four-stage retrofit compressor stability map for first mode stiffness.

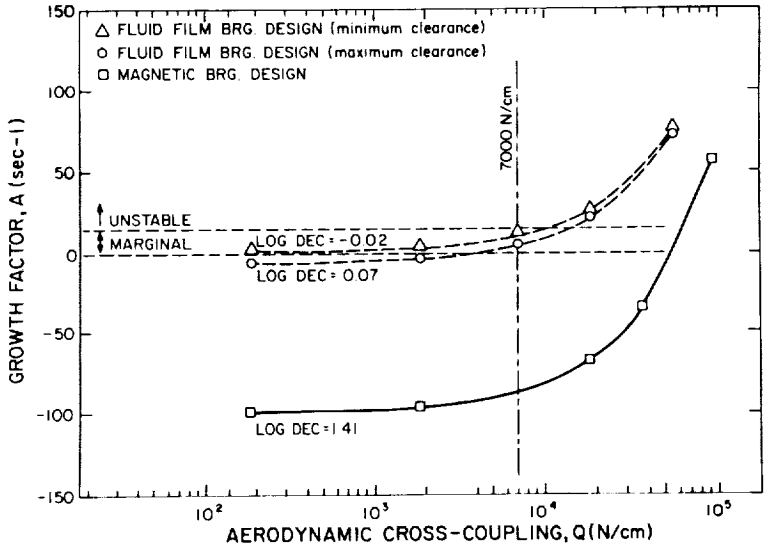

Figure 17. Four-stage retrofit compressor stability analysis results.